Supplementary Methods

Endotoxemia model of sepsis

We injected 8 to 12 week-old C57BL/6 mice with intraperitoneal (IP) LPS (10 µg/g body weight in 50 µl saline; Sigma Aldrich, St. Louis, MO) or saline alone, followed by 1 ml subcutaneous warmed saline for volume resuscitation (allowing for hyperdynamic sepsis). In a separate group of experiments, we induced endotoxemia as above and administered IP 7,8 dihydroxyflavone (5 µg/g in 50 µL DMSO with 20% cyclodextrin, Sigma-Aldrich, St. Louis, MO), a potent tyrosine receptor kinase B agonist, once every 24 hours from days 0 to 6.

Cecal ligation and puncture model of sepsis

We performed cecal ligation and puncture as previously described (1). Briefly, under isoflurane anesthesia, we externalized the cecum via midline incision, used 2:0 silk suture to ligate 50% of the cecal length, punctured the ligated cecum through-and-through with a 23-gauge needle, and reinternalized the cecum. We closed the incision with 2:0 silk suture. We used sham mice (in which the cecum is exposed then immediately reinternalized) as controls. We administered subcutaneous warmed saline (1 ml) for fluid resuscitation and buprenorphine for post-operative analgesia.

Contextual fear conditioning: hippocampal-dependent memory assessment

We used hippocampal contextual fear conditioning, as previously described (2, 3), to assess the cognitive effects of endotoxemia. Seven days after either IP saline injection or LPS injection, animals were subjected to a conditioning session. The testing apparatus consisted of a clear fear-conditioning chamber over a shock grid, 16 stainless steel bars connected to a shock generator

(Colbourn Instruments Model H13-15, Whitehall, PA). On day of conditioning, animals were transported to a behavioral testing suite and allowed to habituate in their home cages for at least 10 minutes. They were placed in the fear-conditioning chamber on 2 occasions, separated by approximately 20 minutes, the first of which was to introduce the mouse to the novel environment and to be monitored for baseline evidence of freezing. On the second occasion during the same conditioning session, the animals were monitored for an additional 2 minutes for freezing then a mild foot shock (2 sec, 1 mA) was delivered. Immediately thereafter, the animal was returned to its home cage and home animal housing room. Twenty-four hours later, the animals were brought back to the behavioral suite and again placed in the conditioning chamber. Animals were monitored for 5-minutes and freezing behavior (an index of fearful memory of the foot shock environment) was assessed at 10 second intervals by a blinded observer. Freezing was defined as the absence of movement except for heartbeat and respiration.

Hippocampal slice preparation

Hippocampal slices were prepared from 8 to 12 week-old healthy C57BL/6 mice or experimental C57BL/6 mice (LPS or cecal ligation and puncture-treated mice). Animals were anesthetized with isoflurane and a thoracotomy was performed to expose the heart. The mice were then transcardially perfused with chilled (2-5 °C), oxygenated (95% O_2, 5% CO_2) artificial cerebrospinal fluid (aCSF; composed of 126 NaCl, 2.5 KCl, 26 $NaHCO_3$, 1.3 NaH_2PO_4, 2.5 $CaCl_2$, 1.2 $MgCl_2$, and 12 glucose, all in mmol/L; all subsequent methods requiring aCSF utilized the same O_2/CO_2 percentages) for 2 minutes. The mice were then decapitated, brains were extracted and transferred to chilled aCSF. Three-hundred μm axial slices were cut using a

Leica 1200VTS vibratome (Wetzlar, Germany) and placed in a holding chamber in room temperature aCSF and allowed to equilibrate for one hour prior to starting recordings.

Hippocampal electrophysiology

Evoked field potentials were recorded as previously described by our group (2, 4). Briefly, 300 µm hippocampal slices were transferred to a temperature controlled (31 +/- 0.5 °C) slice interface chamber and perfused continuously with aCSF. A stimulating platinum bipolar microwire electrode was then placed in the Schaffer collaterals of the Cornu Ammonis Region 3 (CA3) and a glass recording electrode was placed in the stratum radiatum of the Cornu Ammonis Region 1 (CA1) region of the hippocampus. Slices were stimulated to generate field excitatory post-synaptic potentials (fEPSP) every 20 seconds. Stimulus intensity was adjusted to 50% of the maximum fEPSP slope. For control slices, a 20-minute stable baseline signal was established; whereas, for slices perfused with heparan sulfate octasaccharides with or without 7,8 dihydroxyflavone (7,8 DHF; 5mM aliquots in DMSO, diluted to final concentrations in aCSF) or the heparan sulfate antibody 10e4 (aCSF as diluent; clone F58-10e4, Amsbio, Cambridge, MA), a 30 to 60-minute period of baseline recording was performed to allow for equilibration of the treatment with the hippocampal tissue, at which time a 20 minutes baseline recording was performed. When Brain-Derived Neurotrophic Factor (BDNF, aCSF as diluent; catalog number 450-02, Peprotech, Rocky Hill, NJ) was utilized, recordings were started immediately. Subsequently in all paradigms, a theta-burst stimulus (TBS) train of four pulses at 100 Hz in 30-ms bursts repeated 10 times with 200-ms interburst intervals. After TBS, fEPSPs were recorded for an additional 60 minutes.

Analog signals were acquired in real-time and amplified (1000x) and filtered by a pre-amplifier (Model LP511 AC, Grass Instruments, West Warwick, RI) at 0.03 Hz to 1 kHz and digitized. Signals were analyzed off-line in Clampfit (Axon Instruments, San Jose, CA). The fEPSP slope was measured and the averaged slope from the final 10 minutes of recording was divided by the average 10-minute baseline prior to TBS to calculate percent change from baseline. Time course graphs were created by plotting the fEPSP slope averaged over one-minute intervals for both pre and post-TBS recordings expressed as percentage of pre-TBS baseline (set to 100%). Each n represents a single slice and no more than 3 recordings were performed per mouse. For 7-day post-LPS experiments, at least 4 animals were used for each group.

Western blot

Mice were anesthetized with isoflurane and decapitated. Brains were removed, and bilateral hippocampi were then isolated and flash frozen using dry ice. Western analysis was performed as detailed previously (5). Briefly, isolated hippocampi were homogenized in N-Per (Thermo Fisher Scientific, Waltham, MA) with protease and phosphatase inhibitors, lysate was centrifuged at 5,000g and supernatant collected. Protein was quantitated (Biorad DC protein assay, Hercules, CA). Proteins (30µg/lane) were separated on a gradient gel (Novex Bolt 4-12% with MES buffer, Invitrogen, Carlsbad, CA), transferred to a PVDF membrane and incubated overnight with Primary antibody (BDNF, Abcam Ab205067, Cambridge, UK and ß-actin, Cell Signaling Technology 4967S, Danvers, MA) in blocking solution (StartingBlock (TBS) blocking buffer, Thermo Fisher Scientific) overnight. Blots were rinsed, incubated with HRP conjugated secondary antibody, and detected using ECL Western Blotting Detection Reagents (Amersham,

Little Chalfont, UK). Band intensity was quantitated using ImageJ software (National Institutes of Health, Bethesda, MD).

BDNF Enzyme-Linked Immunosorbent Assay

For hippocampal isolation, mice were anesthetized with isoflurane and transcardially perfused with cold phosphate-buffered saline (PBS). Mice were decapitated and hippocampi were isolated then immediately flash frozen. The assay (Mouse BDNF ELISA kit LS-F2404, LSBio, Seattle, WA) was then performed according to the manufacturer's instructions.

Glycosaminoglycan isolation and analysis

We isolated plasma glycosaminoglycans and performed mass spectrometry (LC-MS/MS) multiple reaction monitoring as previously described (5, 6). For hippocampal analysis by LC-MS/MS, mice were anesthetized with isoflurane, transcardially perfused for 5 minutes with cold PBS then immediately decapitated. Bilateral hippocampi were isolated, flash frozen, and stored at -80°F. Brain samples were first defatted overnight with 1 mL 1:1 methanol chloroform mixture. Then the defatted samples were proteolyzed by adding the same dry weight amount of actinase E (10 mg/mL) for 36 h at 55 °C. After the proteolysis, GAGs were purified through Viva pure Q Mini H strong anion exchange spin columns (Sartorius Stedim, Bohemia, NY). Samples eluted from the spin columns were desalted by passing through a 3 kDa molecular weight cut off (MWCO) spin column and washed three times with distilled water. The digestion was performed in a 3 kDa MWCO spin column, 200 μL of digestion buffer (50 mM ammonium acetate containing 2 mM calcium chloride adjusted to pH 7.0) was added to the filter unit. Recombinant heparin lyase I, II, III (pH optima 7.0−7.5) and recombinant chondroitin lyase

ABC (10 mU each, pH optimum 7.4) were added to each sample and mixed well. The samples were all placed in a water bath at 37 °C for 12 h, after which disaccharides were collected by centrifugation. The filter unit was washed twice with 250 μL distilled water and the filtrates containing the disaccharide products were dried via lyophilization. Glycosaminoglycan analysis was then performed by LC-MS/MS multiple reaction monitoring as referenced above. Heparan sulfate content of hippocampi was normalized to weight of extracted tissue in grams, which was recorded at the time of hippocampal isolation.

Confocal microscopy of fresh hippocampal sections

Heparan sulfate was tagged with fluoresceinamine (Sigma, St. Louis, MO) following the activation of heparan sulfate hydroxyl groups with CNBr, pH 11, using a modified protocol from the literature (7). Fluorescein tagged heparan sulfate was purified using ultrafiltration (MWCO, 10,000) and Sephadex G25 chromatography to obtain fluorescein-labeled heparan sulfate free of fluoresceinamine. Fluorescein-labeled heparan sulfate octasaccharide was prepared from the controlled partial heparin lyase III treatment of fluorescein-tagged heparan sulfate followed by size fractionation using P10 column.

Twenty-four hours after intraperitoneal LPS (or saline), we injected 250 μg of fluorescein-conjugated heparan sulfate octasaccharides by tail vein. We used animals not injected with fluorescein-conjugated heparan sulfate injection as controls for background autofluorescence. At least three animals were included in each arm. We sacrificed animals one hour after heparan sulfate injection and systemically infused (via intracardiac puncture) aCSF for 2 minutes, followed by isolation of 200 μm coronal hippocampal slices as described above in **Hippocampal**

slice preparation. Slices including the hippocampus were then immediately mounted on glass slides and allowed to dry for 20 minutes. After drying, hippocampi were mounted in VECTASHIELD Antifade Mounting Media with 4', 6-Diamidine-2'-phenylindole dihydrochloride (DAPI; VECTOR laboratories, Burlingame, CA). The bilateral CA1 cell layers of each slice were visualized using an Olympus 1200 confocal microscope (Tokyo, Japan) at 10x magnification. We analyzed images in a blinded fashion using ImageJ to quantify fluorescein content in the dendritic tree of the CA1 cell layer. Fluorescein intensity was averaged across images (2 to 8 images per animal) from each animal and a comparison was made between treatment arms.

Intravital Microscopy

We anesthetized mice with isoflurane and implanted a skull window (#1 round coverslip, Bellco) allowing visualization of subcortical microvessels as previously described (8). Seven days after window placement, a time point at which animals had completely recovered from surgery, we performed CLP or a sham operation. Twenty-four hours after the operation, animals underwent dual external jugular catheter placement, one for continuous anesthetic infusion (xylazine and ketamine) and the other for injection of tetramethylrhodamine-labeled (TRITC) high molecular weight dextran (150 kDa; Sigma, St Louis, MO) and fluorescein-conjugated heparan sulfate octasaccharides. The animals were then placed under a Nikon A1R high-speed confocal microscope (Tokyo, Japan) directly overlying the implanted brain window to visualize these fluorophore-labeled molecules in the cortical vasculature and parenchyma. We utilized a Nikon 25x CFI APO LWD objective (working distance 2 mm) to maximize cortical penetration. TRITC Dextran (100 μL, 1% dextran in phosphate-buffered saline) was first injected to visualize the

vasculature as it remains in the vascular compartment because of size exclusion by the blood-brain barrier. The fluorescein-heparan sulfate fragments (300 μg) were then injected and images were taken at time of injection and then at 5-minute intervals for a total duration of 30 minutes. Representative images are shown in **Supplementary Figure 3**.

Surface Plasmon Resonance

Surface plasmon resonance measures of heparan sulfate-BDNF binding were measured, as previously described (5). As above, BDNF was purchased from Peprotech (Rocky Hill, NJ). The GAGs used were porcine intestinal heparin (16 kDa) and porcine intestinal heparan sulfate (HS) (12 kDa, Celsus Laboratories, Cincinnati, OH). *N*-desulfated heparin (14 kDa) and 2-*O*-desulfated IdoA heparin (13 kDa) were all prepared based on Yates et al (9). 6-*O*-desulfated heparin (13 kDa) were purchased from Iduron (Manchester, UK). Heparin oligosaccharides included tetrasaccharide (dp4), octasaccharide (dp8), and octadecasaccharide (dp18) were prepared from controlled partial heparin lyase 1 treatment of bovine lung heparin (Sigma) followed by size fractionation. Sensor SA chips were from BIAcore (Biacore AB, Uppsala, Sweden). SPR measurements were performed on a BIAcore 3000 operated using BIAcore 3000 control and BIAevaluation software (version 4.0.1).

Glycoarray

Human BDNF Alexa 488-conjugated antibody was purchased from R & D systems (catalog number IC2481G, Minneapolis, MN). ProBDNF was purchased from Biovision (catalog number 4273, Atlanta, GA). The heparan sulfate antibody, 10e4, was supplied by Amsbio (clone F58-10e4, Cambridge, MA). Heparan sulfate oligosaccharides were prepared through a three-step

reaction as previously described (10). The labeling of human antithrombin (AT; Cutter Biological) and recombinant human platelet factor 4 (PF4; ChromaTec, Greifswald, Germany) was completed by incubating recombinant proteins (AT or PF4, 0.1 mg mL^{-1}) and heparin (0.1 mg/mL) with Alexa Fluor® 488 NHS ester (1 mg/mL, from Invitrogen, Carlsbad, CA) in a 25 mM phosphate buffer (pH 7.0) containing 500 mM NaCl in 3 mL. The reaction was incubated at room temperature for one hour. The reaction mixture was purified by heparin-agarose column (General Electric Health, Chicago, IL) to remove the unreacted Alexa Fluor 488 NHS ester then desalted with Amicon Ultra centrifugal filters with a MWCO of 10 kDa.

Microarrays were printed by sciFLEXARRAYER S5 with various amine-containing heparan sulfate oligosaccharide (50 μM) in print buffer (50 mM phosphate, pH 8.5 containing 0.005% Tween-20) onto *N*-hydroxysuccinimide (NHS)-activated glass slides. Each compound was printed as a 6 × 6 pattern. Printed slides were allowed to react in an atmosphere of 80% humidity for 24 h and non-bonded heparan sulfate oligosaccharides were removed from slides by rinsing with deionized water. Remaining NHS groups were blocked by immersion in buffer (50 mM ethanolamine in 50 mM borate buffer, pH 9.2) for 1 hour at 50 ºC. Slides were rinsed with water, dried, and stored before use.

Printed slides were analyzed without any further modification of the surface. Slides were incubated in a sandwich procedure, in which the protein of interest (i.e. BDNF, 10e4 antibody, PF4, AT) was incubated first, followed by a secondary antibody incubation (10e4 secondary, catalog number A21042, Life Technologies Corporation, Carlsbad, CA; ProBDNF secondary, sc65513, Santa Cruz Biotechnology, Dallas, TX). Primary and secondary antibodies (if

applicable) were added at a concentration of 10 μg/mL in buffer (PBST, 20 mM Tris, 10% BSA). The samples (100 μl) were applied directly onto the surface of a single slide and covered with a microscope slide cover and then incubated in a humidified chamber for 60 minutes. Slides were subsequently washed by successive rinses in (i) PBST, 20 mM Tris, 1% BSA and (ii) deionized water, dried and then immediately imaged. The images were acquired using the excitation wavelength of 488 nm on GenePix 4300 A scanner (Molecular Devices, San Jose, CA). The intensity data is the mean value ± S.D. of 36 individual spots and binding affinity was divided into either high or low affinity. The sulfation quantity and subtype of high versus low affinity heparan sulfate fragment subtypes were compared. The 52 printed heparan sulfate sequences have been previously reported (11).

Neurocognitive Assessment in MESSI Cohort

Twenty patients admitted to the medical intensive care unit (ICU) at the Hospital of the University of Pennsylvania were enrolled in the Neurocognitive Impairment in Respiratory Failure and Shock (NIRFS) study, a sub study of the Molecular Epidemiology of Sepsis in the ICU (MESSI) cohort, which has been described previously (12, 13). Inclusion criteria were sepsis as defined by Sepsis-3 criteria, and either respiratory failure or shock as defined by a cardiovascular or respiratory sequential organ failure assessment score (SOFA) ≥ 3 (14, 15). Patients were excluded if they had preexisting cognitive impairment, an acute neurologic insult (stroke, seizure, cardiac arrest, etc.), neurologic infection, neurologic malignancy, cirrhosis with hepatic encephalopathy, active substance abuse, severe psychiatric disorder, prior ICU stay lasting more than 48 hours in the past 3 months, were transferred from an outside hospital ICU, or had limitations on care. Residual plasma was collected from clinical blood draws at the time

of ICU admission (day 0), day 2 and day 7, and stored at -80°C until analysis. Cognitive function was assessed using the Montreal Cognitive Assessment (MoCA) at hospital discharge or 14 days after ICU discharge in patients who required prolonged hospitalization but had otherwise recovered from sepsis. We defined normal cognitive function as a MoCA score ≥ 26, mild cognitive impairment as a MoCA score 21-25, and moderate to severe cognitive impairment as a MOCA score < 21 (16, 17). Trained research personnel collected clinical data using structured case report forms with standardized definitions. Acute Physiology and Chronic Health (APACHE) III scores were calculated using data from the first 24 hours of ICU admission (18). Acute respiratory distress syndrome was defined within the first 6 days of ICU admission using the Berlin definition with the added requirement of invasive mechanical ventilation(19). This study was approved by the University of Pennsylvania Institutional Review Board with a waiver of timely informed consent (Protocols 808542 and 820585). Informed consent was obtained from patients or their surrogates as soon as feasible, and patients or their surrogates could withdraw from the study at any time.

Supplementary Table 1: Plasma Heparan Sulfate Disaccharide Analyses

	TriS	NS6S	NS2S	NS	2S6S	6S	2S	0S	Total
Mouse Plasma (ng/ml, mean +/- SEM**)**									
Day 0 (n = 9)	0.16 +/- 0.03	0.52 +/- 0.12	0.44 +/- 0.14	0.61 +/- 0.35	1.22 +/- 0.59	0.36 +/- 0.08	0.03 +/- 0.02	70.53 +/- 6.71	74.49 +/- 6.75
Day 1 (n = 6)	0.23 +/- 0.06	1.62 +/- 0.27	4.81 +/- 1.20	7.36 +/-3.44	1.73 +/- 0.72	0.36 +/- 0.11	0.05 +/- 0.04	244.37 +/- 34.34	260.53 +/- 36.57
Day 2 (n = 5)	0.41 +/- 0.07	0.53 +/- 0.15	0.90 +/- 0.35	3.46 +/- 1.51	1.22 +/- 0.59	0.15 +/- 0.08	0.03 +/- 0.02	118.93 +/- 26.80	125.62 +/- 27.86
Day 7 (n = 3)	0.15 +/- 0.05	0.57 +/- 0.26	0.81 +/- 0.36	1.89 +/- 1.05	0.39 +/- 0.10	0.52 +/- 0.41	0.01 +/- 0	41.88 +/- 7.70	46.22 +/- 8.21
Human Plasma (ng/ml, mean +/- SEM**)**									
Normal Donors (n = 9)	0.16 +/- 0.06	0.38 +/- 0.15	0.31 +/- 0.18	0.50 +/- 0.16	0.26 +/- 0.26	0.00 +/- 0.00	0.00 +/- 0.00	21.15 +/- 1.98	22.67 +/- 2.25
Sepsis Day 0 (n = 20)	1.88 +/- 0.87	8.31 +/- 2.49	13.39 +/- 2.45	28.74 +/- 5.35	0.16 +/- 0.8	18.09 +/- 6.06	0.37 +/- 0.08	151.54 +/- 19.68	222.48 +/- 33.34
Sepsis Day 2 (n = 20)	2.03 +/- 1.69	5.49 +/- 1.57	13.73 +/- 2.58	22.33 +/- 3.55	0.15 +/- 0.09	9.45 +/- 1.70	0.13 +/- 0.05	134.23 +/- 16.15	187.53 +/- 21.63
Sepsis Day 7 (n = 19)	9.39 +/- 7.16	9.09 +/- 4.68	22.46 +/- 9.61	32.52 +/- 9.48	0.56 +/- 0.37	12.80 +/- 4.91	1.06 +/- 0.89	193.08 +/- 28.82	280.96 +/- 62.79

Supplementary Table 2: Hippocampal Heparan Sulfate Disaccharide Analyses

	TriS	NS6S	NS2S	NS	2S6S	6S	2S	0S	Total
Mouse Hippocampus (ng/gm tissue, mean +/- SEM**)**									
Day 0 (n = 3)	46.21 +/- 13.00	212.01 +/- 26.40	782.58 +/- 81.20	2065.59 +/- 178.02	5.01 +/- 1.67	437.72 +/- 55.35	25.50 +/- 12.63	13149.47 +/- 388.03	16724.08 +/- 355.97
Day 1 (n = 3)	122.79 +/- 49.69	497.01 +/- 140.86	1774.15 +/- 412.38	3844.11 +/- 443.54	19.56 +/- 1.88	971.73 +/- 188.45	67.94 +/- 10.18	17319.41 +/- 951.62	24621.70 +/- 1892.64
Day 7 (n = 3)	156.10 +/- 3.48	658.26 +/- 16.87	1988.58 +/- 32.10	3975.72 +/- 174.63	21.09 +/- 4.17	1242.17 +/- 84.16	44.81 +/- 4.77	16164.05 +/- 548.12	24250.78 +/- 599.39

Supplementary Table 3: Heparan Sulfate Disaccharide Analyses (day 0) in patients with mild/no or moderate/severe cognitive impairment (hospital discharge or day 14 post-ICU)

HS Fragment		Mild or No Cognitive Impairment	Moderate or Severe Cognitive Impairment	p
Day 0	2SNS6S	0.135 (0-0.4)	0.45 (0-10.76)	0.2329
	NS6S	1.66 (0.49-3.89)	19.935 (1.62-32.11)	0.0908
	NS2S	**5.675 (2.41-10.78)**	**25.09 (13.63-30.18)**	**0.0478**
	NS	13.1 (7.86-25.13)	43.005 (24.4-77.71)	0.0696
	S2S6S	0.0 (0.0-0.08)	0.175 (0.0-0.033)	0.1135
	S6S	2.97 (0.0-9.49)	23.765 (0.0-66.06)	0.2772
	S2S	0.12 (0.07-0.35)	0.34 (0.0-0.8)	0.5606
	0S	111.78 (81.43-181.44)	179.38 (146.61-287.2)	0.1376
	Total HS	149.265 (93.97-231.6)	343.745 (187.28-453.02)	0.0833
	Total NS	**23.87 (11.86-39.17)**	**101.6 (39.65-137.34)**	**0.0578**
	NS + NS2S + NS6S	**23.665 (11.21-31.85)**	**90.665 (39.65-136.87)**	**0.0478**
Day 2	2SNS6S	0.05 (0.0-0.52)	0.13 (0.0-0.45)	0.6652
	NS6S	1.56 (0.46-5.88)	5.04 (2.55-9.02)	0.1609
	NS2S	7.505 (4.12-15.6)	16.0 (6.47-20.76)	0.3223
	NS	11.995 (7.37-35.0)	27.56 (15.72-35.89)	0.1868
	S2S6S	0.0 (0.0-0.08)	0.0 (0.0-0.0)	0.7450
	S6S	5.145 (1.8-13.45)	7.2 (5.16-13.72)	0.5092
	S2S	0.05 (0.0-0.31)	0.0 (0.0-0.0)	0.1033
	0S	106.42 (66.83-169.22)	169.215 (117.12-191.12)	0.3223
	Total HS	141.075 (91.97-270.7)	232.83 (186.83-241.63)	0.1869
	Total NS	22.795 (11.71-61.32)	54.665 (34.63-81.73)	0.1869
	NS + NS2S + NS6S	20.91 (11.71-61.32)	54.375 (34.63-69.12)	0.2160
Day 7	2SNS6S	0.43 (0.1-3.78)	0.075 (0.0-0.89)	0.2097
	NS6S	2.54 (0.35-8.72)	1.995 (0.74-3.2)	0.8046
	NS2S	12.01 (3.39-26.7)	5.275 (3.39-11.01)	0.2009
	NS	26.89 (8.85-32.48)	19.47 (7.32-29.56)	0.4579
	S2S6S	0.0 (0.0-0.32)	0.0 (0.0-0.0)	0.0672
	S6S	8.69 (3.3-15.18)	5.62 (3.64-8.14)	0.5631
	S2S	0.025 (0.0-0.61)	0.0 (.0-0.15)	0.4701
	0S	161.445 (117.22 – 253.09)	202.63 (85.54-210.41)	0.7415
	Total HS	250.955 (131.14-342.42)	243.49 (94.62-259.8)	0.4579
	Total NS	42.195 (12.45-104.93)	29.515 (14.61-41.89)	0.3223
	NS + NS2S + NS6S	41.945 (12.45-89.29)	29.515 (13.61-41.89)	0.3223

Supplementary Figures

Supplementary Figure 1. A. Intraperitoneal LPS (10 μg/g body weight) confers an 18% mortality, with the majority of animals dying within 72 hours of injection. n = 54 mice (LPS), n = 46 mice (Saline). **B.** Sickness behavior (including lethargy and weight loss) peaks 2 days after intraperitoneal LPS (10 μg/g body weight). By 7 days after intraperitoneal LPS, mouse activity has normalized with resumption of weight gain. ** $p < 0.01$; * $p < 0.05$ compared to contemporaneous intraperitoneal saline control by t-test. n = 7 mice (LPS), 6 mice (saline).

Supplementary Figure 2. Hippocampal BDNF levels are unchanged seven days after sepsis. Hippocampal BDNF content is not different one week after endotoxemia, when compared to saline injected controls as assessed with a BDNF-specific ELISA. n = 5 control, n = 6 LPS. Statistical analysis by t-test, $p = 0.52$.

Supplementary Figure 3. FITC-heparin octasaccharides rapidly extravasate from superficial cortical microvessels. 1 week after skull window placement, 8 to 12 week-old C57BL/6 mice underwent cecal ligation and puncture (CLP) or sham surgery. 24 h later (a timepoint associated with circulating heparan sulfate), we performed brain intravital high-speed confocal microscopy and administered both 250 μg fluorescein-labeled highly-sulfated heparan sulfate (heparin) octasaccharides and 100 μl 1% TRITC-dextran (150 kDa, an intravascular marker). Intravital imaging was performed using a Nikon 25x CFI APO LWD objective (1.1 numerical aperture), which has a working distance of 2 mm. As such, images likely reflect superficial cortical vessels. While heparin octasaccharides are primarily intravascular immediately after injection (time = 1 minute), they rapidly diffuse out of the vasculature in both

septic and non-septic mice. Images representative of 3 biological replicates per group. Scale bar 20 μm.

Supplementary Figure 4. Hippocampal heparan sulfate and cognition 14 days after LPS. **A**. Total hippocampal heparan sulfate and (**B**.) disaccharide subtype content normalizes in comparison to contemporaneous controls 14 days after endotoxemia, coincident with (**C**.) normalization of hippocampal-dependent memory as measured by contextual fear conditioning. Statistical analyses by t-test (**A**, **C**) or t-test for single comparisons (**B**). * $p < 0.05$. Saline n = 6 (**A, B**) or 12 (**C**), LPS n = 6 (**A, B**) or 16 (**C**).

Supplementary Figure 5. Heparan sulfate binding to BDNF is size- and sulfation-dependent. A. Surface plasmon resonance demonstrates that highly-sulfated heparan sulfate (HS, as modeled by heparin) fragments must be at least octasaccharides in size to bind brain-derived neurotrophic factor (BDNF). **B.** Similarly, selectively-desulfated HS demonstrates the relative importance of *N*, 6-*O*, and 2-*O* sulfation to HS-BDNF binding. Notably, circulating HS fragments in sepsis are typically highly-sulfated octasaccharides (reference 14 of the main manuscript). dp = degree of polymerization. n = 3/group. * $p < 0.05$ by ANOVA.

Supplementary Figure 6. Heparan sulfate glycoarray analysis identifies BDNF-avid sulfation sequences. A. BDNF was applied to an array of 52 different heparan sulfate oligosaccharides. After washing, a BDNF-specific antibody was used to identify which oligosaccharides bound BDNF, as defined by (**B.**) fluorescent intensity of >2500 arbitrary units.

C. This approach revealed 12 high-affinity BDNF-binding sequences. * = high affinity sequences.

Supplementary Figure 7. Mass spectrometry multiple reaction monitoring (MRM) analyses of sulfation patterns of circulating heparan sulfate in patients with sepsis. Analyses demonstrate that circulating (**A.**) all-NS (NS, NS2S, NS6S, TriS), (**B.**) all-6S (6S, 6S2S, NS6S, TriS), (**C.**) all-2S (2S, 6S2S, NS2S, TriS), and (**D.**) unsulfated heparan sulfate may persist in septic patients for up to 7 days after intensive care unit admission. **** $p < 0.0001$, *** $p < 0.001$, ** $p < 0.01$ by Kruskal-Wallis with Dunn's test for multiple comparisons. n same for all panels.

Supplementary Figure 8: Glycoarray analyses of putative heparan sulfate binding proteins demonstrate the unique sulfation specificity of BDNF. A. Pro-BDNF demonstrated no binding to heparan sulfate oligosaccharides using a glycoarray, suggesting a hidden heparin-binding domain that is revealed when cleaved to become the mature form of BDNF. **B-D.** The heparan sulfate antibody 10e4, antithrombin III, and platelet factor 4 were each evaluated for heparan sulfate binding using a glycoarray. The heparan sulfate oligosaccharides bound by each molecule (quantified for each panel on the right) are distinct from the heparan sulfate-BDNF binding pattern (see **Supplementary Figure 6**).

Supplementary Figure 9: Sequestration of non-BDNF avid heparan sulfate oligosaccharides does not reverse heparan sulfate-induced LTP inhibition. Neutralization of non-BDNF-avid HS sequences with the 10e4 antibody failed to prevent HS-induced loss of LTP,

supporting the sulfation sequence specificity of LTP inhibition by heparan sulfate fragments.

**** $p < 0.0001$ by t-test.

Supplementary References

1. Schmidt EP, et al. The pulmonary endothelial glycocalyx regulates neutrophil adhesion and lung injury during experimental sepsis. *Nat Med.* 2012;18(8):1217-23.
2. Dietz RM, et al. Juvenile cerebral ischemia reveals age-dependent BDNF–TrkB signaling changes: Novel mechanism of recovery and therapeutic intervention. *J Cereb Blood Flow Metab.* 2018;38(12):2223-35.
3. Rudy JW, and O'Reilly RC. Conjunctive representations, the hippocampus, and contextual fear conditioning. *Cogn Affect Behav Neurosci.* 2001;1(1):66-82.
4. Deng G, et al. Autonomous CaMKII Activity as a Drug Target for Histological and Functional Neuroprotection after Resuscitation from Cardiac Arrest. *Cell Rep.* 2017;18(5):1109-17.
5. Yang Y, et al. Fibroblast Growth Factor Signaling Mediates Pulmonary Endothelial Glycocalyx Reconstitution. *Am J Respir Cell Mol Biol.* 2017;56(5):727-37.
6. Sun X, et al. Analysis of total human urinary glycosaminoglycan disaccharides by liquid chromatography–tandem mass spectrometry. *Anal Chem.* 2015;87(12):6220-7.
7. Glabe CG, Harty PK, and Rosen SD. Preparation and properties of fluorescent polysaccharides. *Anal Biochem.* 1983;130(2):287-94.
8. Cabrales P, and Carvalho LJ. Intravital microscopy of the mouse brain microcirculation using a closed cranial window. *J Vis Exp.* 2010(45):2184.
9. Yates EA, Santini F, Guerrini M, Naggi A, Torri G, and Casu B. 1H and 13C NMR spectral assignments of the major sequences of twelve systematically modified heparin derivatives. *Carbohydr Res.* 1996;294:15-27.
10. Yang J, et al. Construction and characterisation of a heparan sulphate heptasaccharide microarray. *Chem Commun (Camb).* 2017;53(10):1743-6.
11. Zhang X, et al. Chemoenzymatic synthesis of heparan sulfate and heparin oligosaccharides and NMR analysis: paving the way to a diverse library for glycobiologists. *Chem Sci.* 2017;8(12):7932-40.
12. Anderson BJ, et al. Admission plasma levels of the neuronal injury marker neuron-specific enolase are associated with mortality and delirium in sepsis. *J Crit Care.* 2016;36:18-23.
13. Reilly JP, et al. ABO blood type A is associated with increased risk of ARDS in whites following both major trauma and severe sepsis. *Chest.* 2014;145(4):753-61.
14. Singer M, et al. The third international consensus definitions for sepsis and septic shock (Sepsis-3). *JAMA.* 2016;315(8):801-10.
15. Vincent JL, et al. The SOFA (Sepsis-related Organ Failure Assessment) score to describe organ dysfunction/failure. On behalf of the Working Group on Sepsis-Related Problems of the European Society of Intensive Care Medicine. *Intensive Care Med.* 1996;22(7):707-10.
16. Freitas S, Simoes MR, Marôco J, Alves L, and Santana I. Construct validity of the montreal cognitive assessment (MoCA). *J Int Neuropsychol Soc.* 2012;18(2):242-50.

17. Nasreddine ZS, et al. The Montreal Cognitive Assessment, MoCA: a brief screening tool for mild cognitive impairment. *J Am Geriatr Soc.* 2005;53(4):695-9.
18. Knaus WA, et al. The APACHE III prognostic system: risk prediction of hospital mortality for critically III hospitalized adults. *Chest.* 1991;100(6):1619-36.
19. Force ADT, Ranieri V, and Rubenfeld G. Acute respiratory distress syndrome. *JAMA.* 2012;307(23):2526-33.

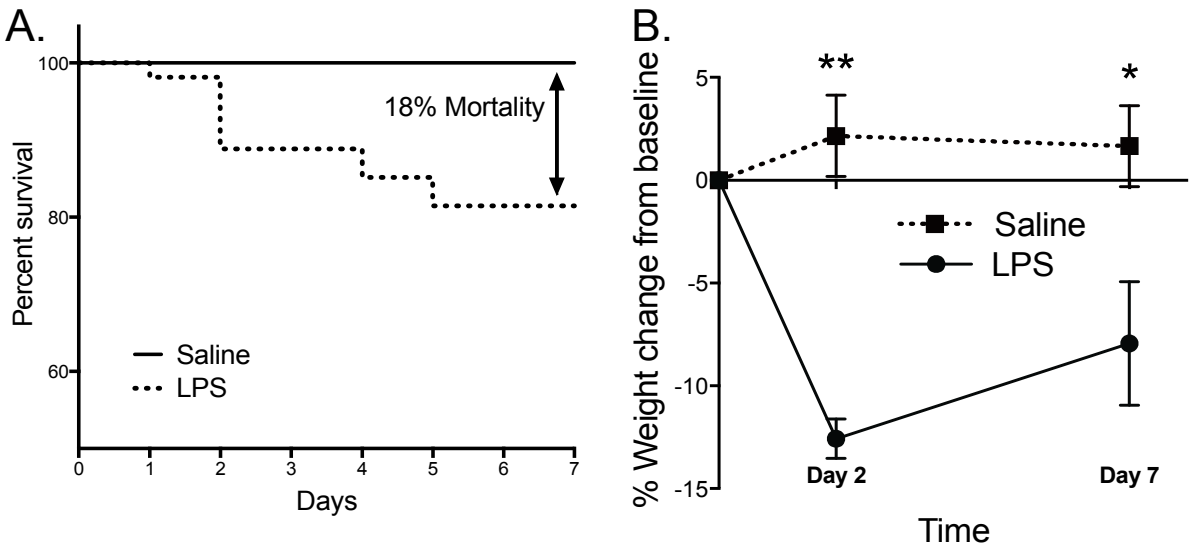

Supplementary Figure 1. A. Intraperitoneal LPS (10 μg/g body weight) confers an 18% mortality, with the majority of animals dying within 72 hours of injection. n = 54 mice (LPS), n = 46 mice (Saline). **B**. Sickness behavior (including lethargy and weight loss) peaks 2 days after intraperitoneal LPS (10 μg/g body weight). By 7 days after intraperitoneal LPS, mouse activity has normalized with resumption of weight gain. ** $p < 0.001$; * $p < 0.05$ compared to contemporaneous intraperitoneal saline control by t-test. n = 7 mice (LPS), 6 mice (saline).

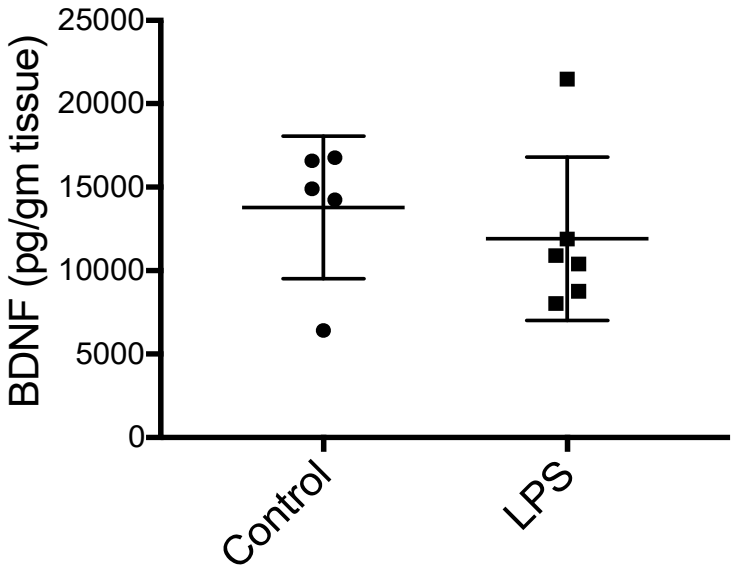

Supplementary Figure 2. Hippocampal BDNF levels are unchanged seven days after sepsis. Hippocampal BDNF content is not different one week after endotoxemia when compared to saline injected controls as assessed with a BDNF-specific ELISA. n = 5 control, n = 6 LPS. Statistical analysis by t-test, p = 0.52.

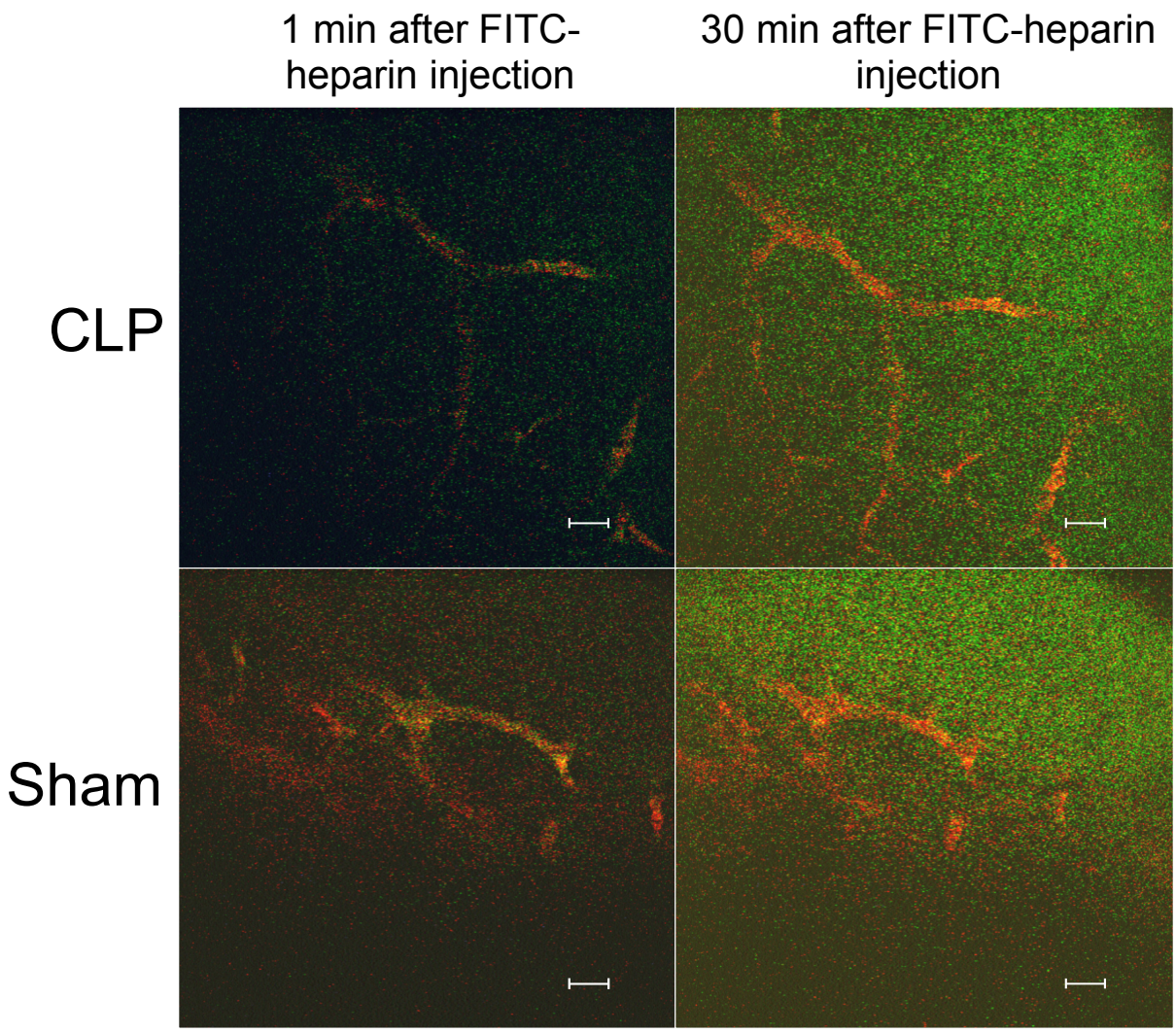

Supplementary Figure 3. FITC-heparin octasaccharides rapidly extravasate from superficial cortical microvessels. 1 week after skull window placement, 8 to 12 week-old C57BL/6 mice underwent cecal ligation and puncture (CLP) or sham surgery. 24 h later (a timepoint associated with circulating heparan sulfate), we performed brain intravital high-speed confocal microscopy and administered both 250 µg fluorescein-labeled highly-sulfated heparan sulfate (heparin) octasaccharides and 100 µl 1% TRITC-dextran (150 kDa, an intravascular marker). Intravital imaging was performed using a Nikon 25x CFI APO LWD objective (1.1 numerical aperture), which has a working distance of 2 mm. As such, images likely reflect superficial cortical vessels. While heparin octasaccharides are primarily intravascular immediately after injection (time = 1 minute), they rapidly diffuse out of the vasculature in both septic and non-septic mice. Images representative of 3 biological replicates per group. Scale bar 20 µm.

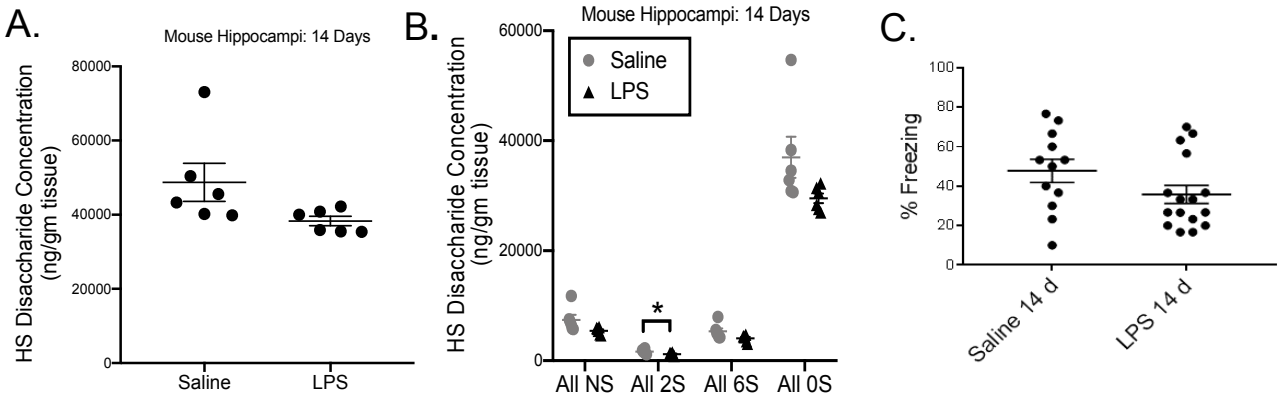

Supplementary Figure 4. Hippocampal heparan sulfate and cognition 14 days after LPS. **A**. Total hippocampal heparan sulfate and (**B**.) disaccharide subtype content normalizes in comparison to contemporaneous controls 14 days after endotoxemia, coincident with (**C**.) normalization of hippocampal dependent memory as measured by contextual fear conditioning. Statistical analyses by t-test (**A, C**) or t-test for single comparisons (**B**). * $p < 0.05$. Saline n = 6 (**A, B**) or 12 (**C**), LPS n = 6 (**A, B**) or 16 (**C**).

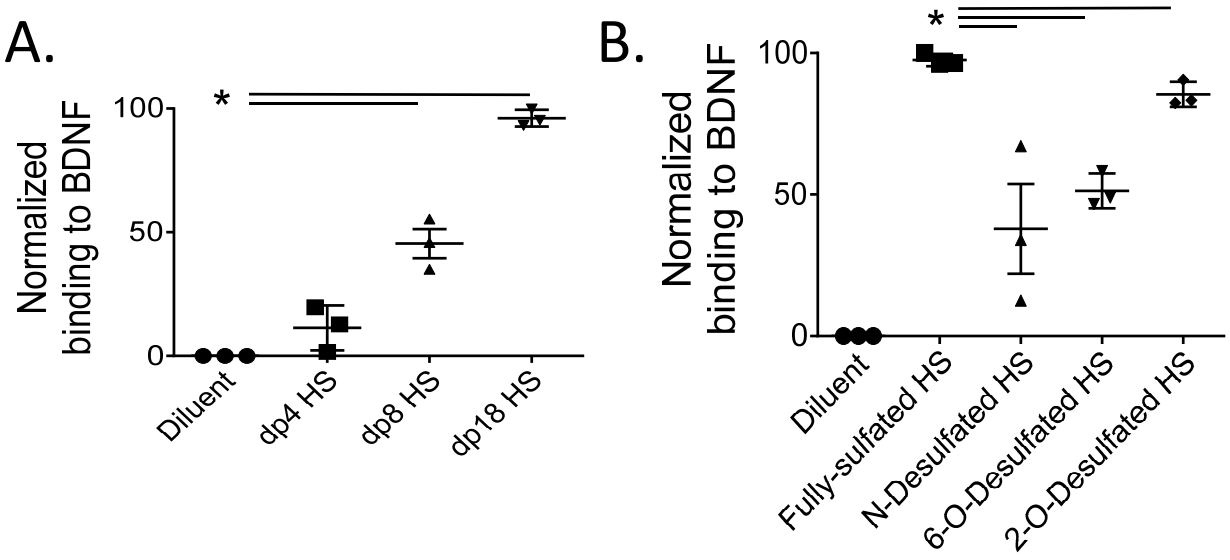

Supplementary Figure 5. Heparan sulfate binding to BDNF is size- and sulfation-dependent. A. Surface plasmon resonance demonstrates that highly-sulfated heparan sulfate (HS, as modeled by heparin) fragments must be at least octasaccharides in size to bind brain-derived neurotrophic factor (BDNF). **B**. Similarly, selectively-desulfated HS demonstrates the relative importance of N, 6-O, and 2-O sulfation to HS-BDNF binding. Notably, circulating HS fragments in sepsis are typically highly-sulfated octasaccharides (reference 14 of the main manuscript). dp = degree of polymerization. n = 3/group. * $p < 0.05$ by ANOVA.

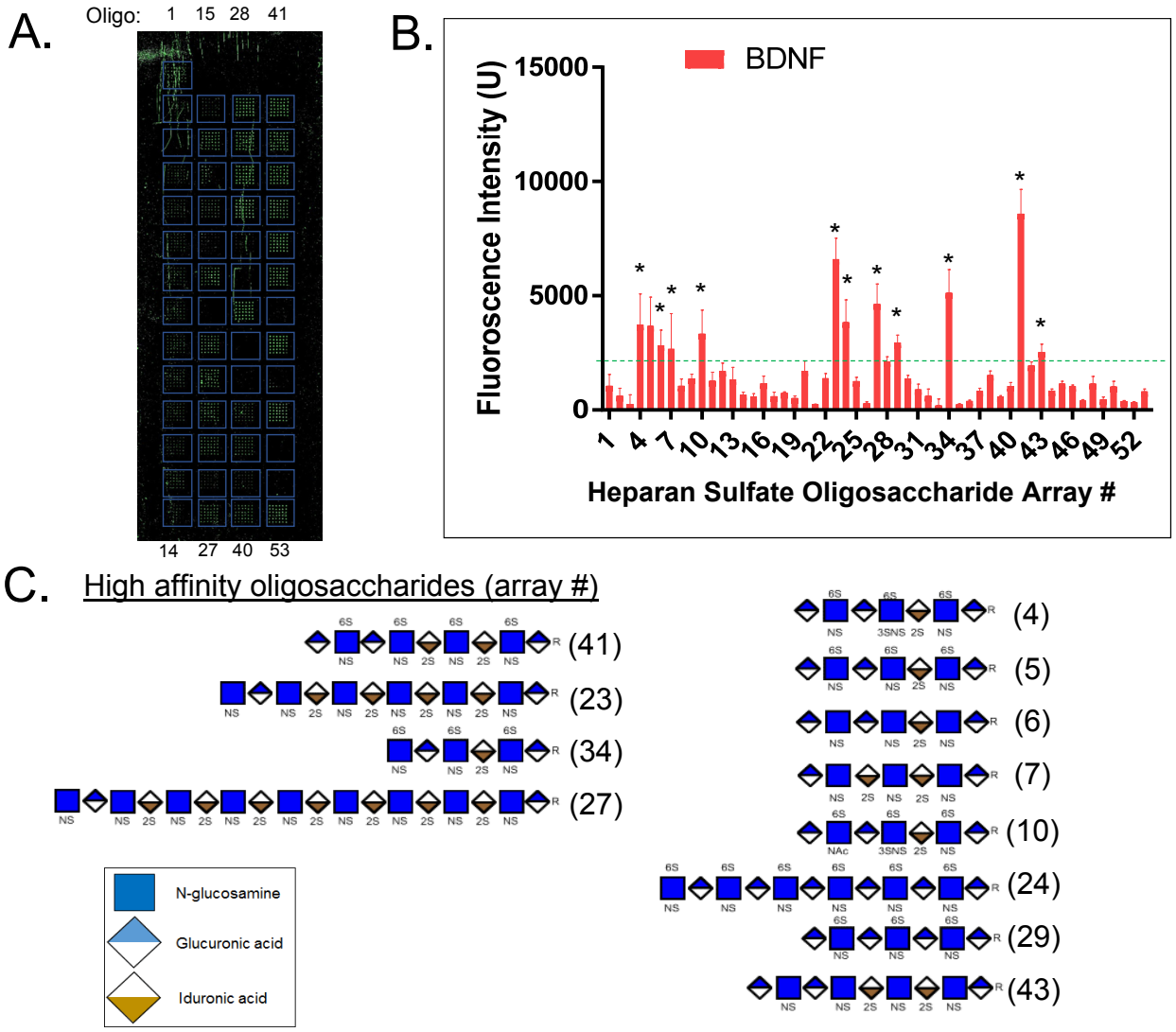

Supplementary Figure 6. Heparan sulfate glycoarray analysis identifies BDNF-avid sulfation sequences. A. BDNF was applied to an array of 52 different heparan sulfate oligosaccharides. After washing, a BDNF-specific antibody was used to identify which oligosaccharides bound BDNF, as defined by (**B**.) fluorescent intensity of >2500 arbitrary units. **C**. This approach revealed 12 high-affinity BDNF-binding sequences. * = high affinity sequences.

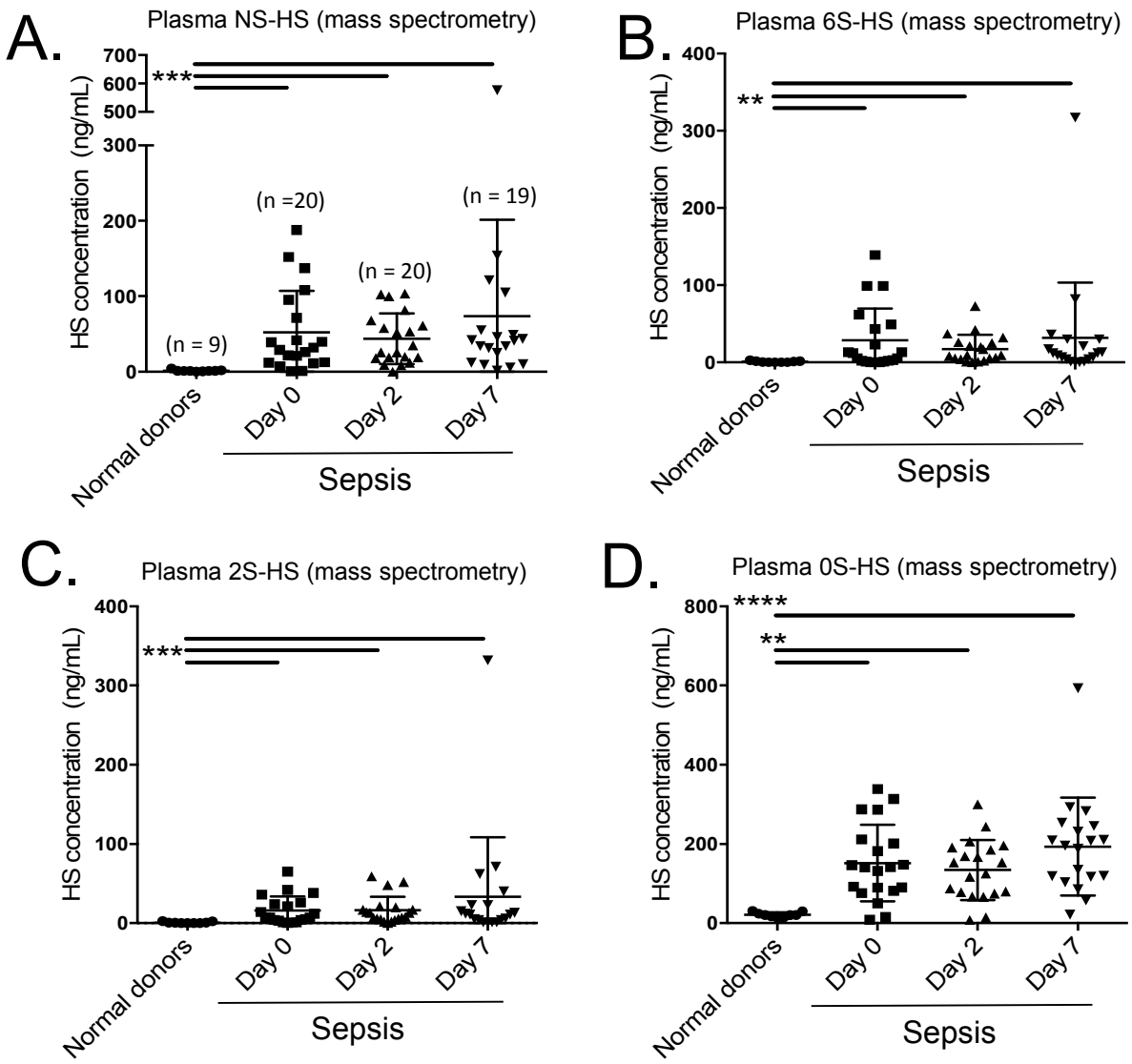

Supplementary Figure 7. Mass spectrometry MRM analyses of sulfation patterns of circulating heparan sulfate in patients with sepsis. Analyses demonstrate that circulating (**A**.) all-NS (NS, NS2S, NS6S, TriS), (**B**.) all-6S (6S, 6S2S, NS6S, TriS), (**C**.) all-2S (2S, 6S2S, NS2S, TriS), and (**D**.) unsulfated heparan sulfate may persist in septic patients for up to 7 days after intensive care unit admission. **** $p < 0.0001$, *** $p < 0.001$, ** $p < 0.01$ by Kruskal-Wallis with Dunn's test for multiple comparisons. n same for all panels.

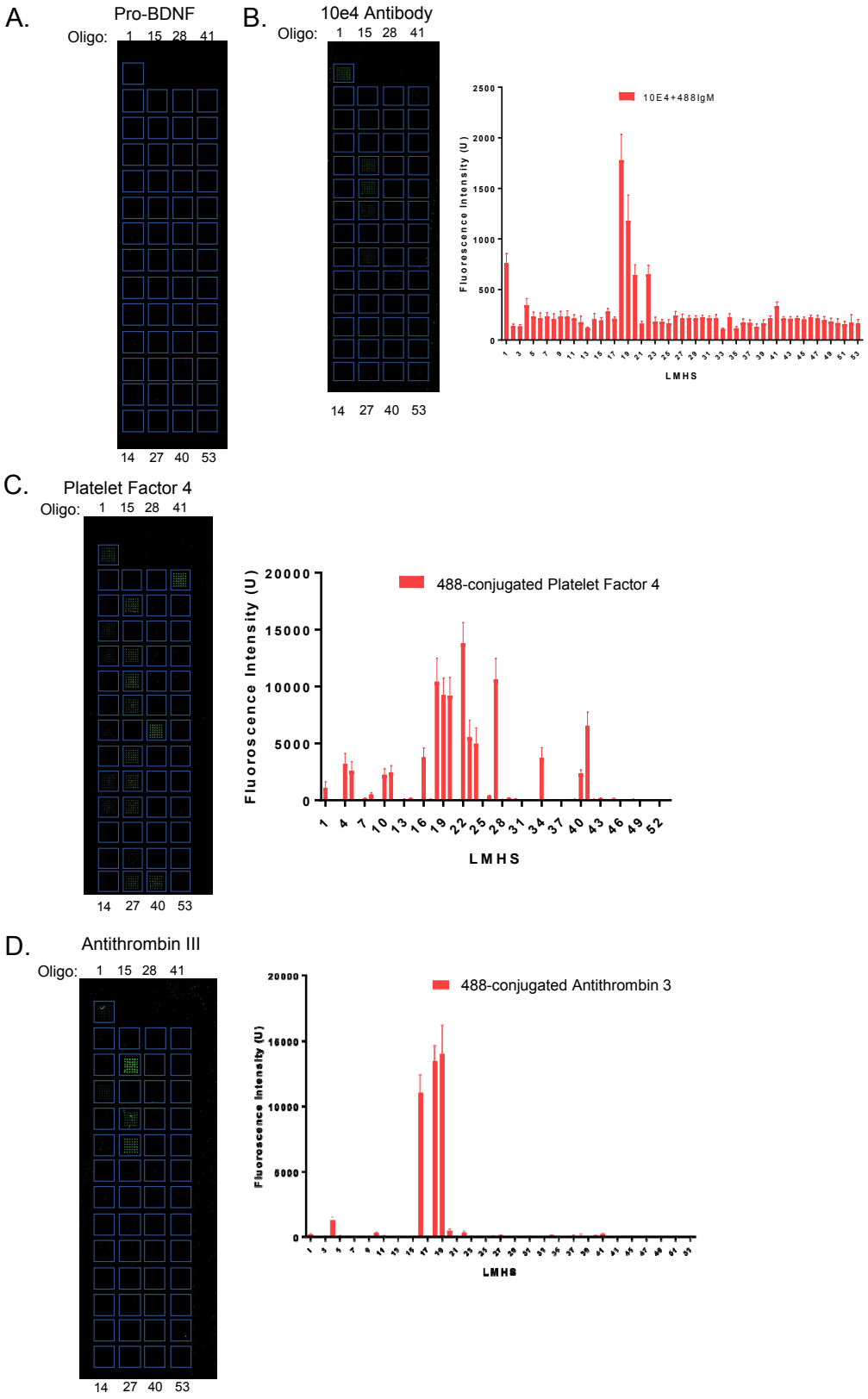

Supplementary Figure 8: Glycoarray analyses of putative heparan sulfate binding proteins demonstrate the unique sulfation specificity of BDNF. A. ProBDNF demonstrated no binding to heparan sulfate oligosaccharides using a glycoarray, suggesting a hidden heparin-binding domain that is revealed when cleaved to become the mature form of BDNF. **B-D**. The heparan sulfate antibody 10e4, antithrombin III, and platelet factor 4 were each evaluated for heparan sulfate binding using a glycoarray. The heparan sulfate oligosaccharides bound by each molecule (quantified for each panel on the right) are distinct from the heparan sulfate-BDNF binding pattern (see **Supplementary Figure 6**).

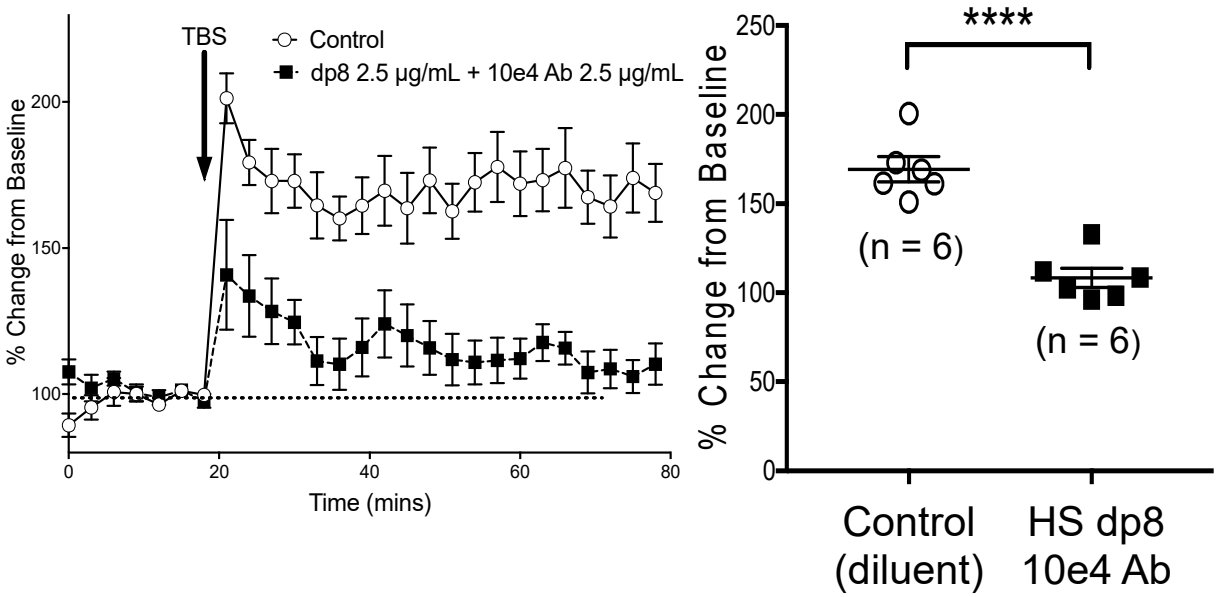

Supplementary Figure 9: Sequestration of non-BDNF-avid heparan sulfate oligosaccharides does not reverse heparan sulfate-associated LTP deficits. Neutralization of non-BDNF-avid HS sequences with the 10e4 antibody failed to prevent HS-induced loss of LTP, supporting the sulfation specificity of LTP inhibition by heparan sulfate fragments. **** $p < 0.0001$ by t-test.